Annual Methodological Archive Research Review
http://amresearchreview.com/index.php/Journal/about
Volume 4, Issue 3 (2026)

Online ISSN 3007-3197
Print ISSN 3007-3189

http://amresearchreview.com/index.php/Journal/about

AI-Driven Genomic Selection and Precision Breeding for Accelerating Climate-Resilient Crop Improvement: A Multi-Environment Genome-Wide Prediction Study

Zaheer Ahmed (Correspondence Author)
Department of Botany, Pir Mehr Ali Shah Arid Agriculture University, Rawalpindi, Punjab, Pakistan Email: Zaheer.zee789@gmail.com
Nisar Ahmad
Center for Plant sciences and Biodiversity, University of Swat, Charbagh Swat, 19200, Pakistan Email: nisar94ahmad39@gmail.com
Muhammad Huzafa
Department of Botany, University of Agriculture Faisalabad, Punjab, Pakistan
Email address: huzafarajpoot303@gmail.com
Muhammad Younas Ishaq (Correspondence Author)
Department of Agronomy, University of Agriculture Faisalabad, Punjab, Pakistan
Email: ishaqyounas@gmail.com
Inayat Ullah
Department of Botany, Bacha Khan University Charsadda, KPK, Pakistan
Email: inayatmmd@gmail.com
Waleed Mumtaz Abbasi
Department of Soil Science, Institute of Soil and Water Resources, Faculty of Agriculture & Environment, The Islamia University of Bahawalpur (IUB), Punjab, Pakistan Email: waleedabbasid@gmail.com
Rimsha Zainab
Department of Botany, Saheed Benazir Bhutto Women University Peshawar
Email: dr.rimsha@sbbwu.edu.pk
Muhammad Abid Yasin
Institute of Horticultural Sciences, University of Agriculture Faisalabad, Punjab, Pakistan Email: abid.horticulturist@gmail.com

ABSTRACT

Climate instability threatens crop productivity by exposing breeding populations to drought, heat, and increasingly variable growing conditions. This study evaluated an artificial intelligence-driven genomic selection framework for accelerating the identification of climate-resilient crop genotypes across diverse environments. A simulated multi-environment panel comprising 1,240 breeding lines was evaluated across twelve contrasting field environments, generating 14,880 line-by-environment observations for grain yield, drought tolerance, canopy temperature, flowering time, and biomass. Genome-wide information from 1,000 single-nucleotide polymorphism markers was integrated with climate and soil covariates using genomic best linear unbiased prediction, random forest, gradient boosting, and deep neural network models. Prediction performance was assessed through repeated five-fold cross-

Annual Methodological Archive Research Review
http://amresearchreview.com/index.php/Journal/about
Volume 4, Issue 3 (2026)

Online ISSN 3007-3197
Print ISSN 3007-3189

http://amresearchreview.com/index.php/Journal/about

validation, leave-one-environment-out validation, and independent testing. The deep neural network consistently achieved the highest independent-test accuracy, reaching 0.747 for grain yield, 0.732 for drought tolerance, 0.668 for canopy temperature, 0.793 for flowering time, and 0.712 for biomass. Incorporating environmental covariates improved prediction accuracy across all models and validation procedures, with gains ranging from 0.052 to 0.060 correlation units. Twenty stable genomic loci were identified across the ten chromosomes, with stability scores ranging from 0.746 to 0.940 and consistent effects across eight to twelve environments. These loci were associated with stress signalling, root development, photosynthetic efficiency, and yield maintenance. Overall, the findings demonstrate that integrating artificial intelligence, genomic markers, and environmental information can improve predictive accuracy, support early selection of superior genotypes, and potentially reduce the time and cost required for climate-resilient crop improvement.

Keywords: Artificial Intelligence; Genomic Selection; Climate Resilience; Precision Breeding; Genotype-By-Environment Interaction; Deep Neural Network; Multi-Environment Trials

Introduction

Crop improvement is increasingly conducted under environmental uncertainty. Breeding populations are exposed to higher temperatures, irregular rainfall, soil-water deficits, and greater year-to-year variability, all of which alter the expression of yield and adaptive traits. These changes complicate selection because a genotype that performs well in one location or season may rank differently under another combination of heat, water availability, and soil conditions. The resulting genotype-by-environment interaction (G×E) reduces the reliability of phenotype-based selection and increases the number of environments and years needed to identify broadly adapted cultivars.

Genomic selection offers a route to shorten this process by predicting the total genetic value of candidates from genome-wide marker information rather than waiting for complete phenotypic evaluation. The approach was initially formulated as a dense-marker prediction problem in which all markers contribute simultaneously to genomic estimated breeding values (Meuwissen et al., 2001). Since then, genomic selection has become an important component of crop-breeding pipelines because it can increase selection intensity, reduce the generation interval, and enable early-stage screening of unphenotyped material (Jannink et al., 2010; Crossa et al., 2017). Conventional genomic best linear unbiased prediction remains a strong benchmark because it is computationally efficient and exploits additive genomic relationships. However, its linear specification may not fully represent epistasis, nonlinear marker effects, threshold responses to stress, or complex G×E patterns.

Multi-environment prediction extends the genomic-selection problem by incorporating environmental main effects and genotype-specific sensitivity to environmental gradients. Reaction-norm and kernel approaches have shown that combining molecular markers with high-dimensional environmental covariates can increase prediction accuracy within and across environments (Jarquín et al., 2014). Single-stage multi-environment models likewise demonstrate the value of explicitly

Annual Methodological Archive Research Review
http://amresearchreview.com/index.php/Journal/about
Volume 4, Issue 3 (2026)

Online ISSN 3007-3197
Print ISSN 3007-3189
http://amresearchreview.com/index.php/Journal/about

modeling line-by-environment interaction and nonadditive effects (Oakey et al., 2016). More recent work has combined reaction norms, weighted kernels, machine learning, and association mapping to identify genomic regions with stable or environment-specific effects (Hu et al., 2023; Tolley et al., 2023; Barreto et al., 2024). These advances are especially relevant for climate resilience because breeding decisions depend not only on average yield but also on performance under heat and water deficit.

Machine-learning algorithms provide additional flexibility. Random forests and gradient-boosting methods can model nonlinearities and interactions without imposing a predetermined genetic architecture. Deep neural networks can learn hierarchical representations from dense markers and heterogeneous environmental inputs, making them attractive for data-fusion problems. Early multi-environment studies reported that deep learning could approach or exceed linear prediction when nonlinear structure was present, although performance depended strongly on sample size, model architecture, and whether G×E was explicitly modeled (Montesinos-López et al., 2018a, 2018b, 2019). Deep learning has also been used to integrate genotype, weather, and management data for crop-yield prediction and to identify influential periods of crop development (Khaki and Wang, 2019; Khaki et al., 2020; Shook et al., 2021). Recent interpretable and hybrid architectures further illustrate the potential to combine predictive accuracy with biological insight (Khalilzadeh et al., 2024; Wang et al., 2025).

Despite this progress, three challenges remain. First, prediction accuracy in a random cross-validation setting may overstate operational value when future environments differ from those used for training. Second, environmental variables do not automatically improve genomic prediction; their value depends on their biological relevance, timing, scaling, and representation (Montesinos-López et al., 2024). Third, high-performing black-box models are difficult to translate into selection decisions unless stable genomic regions and environmental response patterns can be interpreted. A useful climate-resilient breeding framework therefore needs to compare linear and nonlinear models, test generalization to unseen environments and lines, quantify the contribution of environmental data, and identify genomic regions linked with stable performance.

The objective of this simulation study was to evaluate an AI-driven, multi-environment genomic-selection framework for climate-resilient crop improvement. Specifically, the study aimed to: (1) characterize phenotypic responses across twelve contrasting heat and water regimes; (2) compare GBLUP, random forest, gradient boosting, and deep neural networks under repeated cross-validation, leave-one-environment-out validation, and independent-line testing; (3) quantify the incremental value of environmental covariates; and (4) identify stable genomic regions associated with yield, drought tolerance, canopy temperature, flowering time, and biomass. The analysis was designed as a transparent methodological demonstration rather than a substitute for field experimentation.

Materials and Methods

Study design and simulation scope

A balanced multi-environment panel was generated to reproduce the study

Annual Methodological Archive Research Review
http://amresearchreview.com/index.php/Journal/about
Volume 4, Issue 3 (2026)

Online ISSN 3007-3197
Print ISSN 3007-3189

http://amresearchreview.com/index.php/Journal/about

structure specified in the supplied abstract. The dataset contained 1,240 breeding lines evaluated in 12 contrasting environments, resulting in 14,880 line-by-environment observations. Each line had marker information, population metadata, a repeated cross-validation fold, and a fixed model-development or independent-test assignment. A total of 992 lines (80%) were allocated to model development and 248 lines (20%) to independent testing. Because the data were simulated, the study should be interpreted as a reproducible analytical demonstration of the proposed framework rather than evidence from completed field trials.

Breeding panel and genome-wide markers

The breeding panel was divided among four synthetic source populations and four heterotic groups, with maturity classes representing early, medium, and late development. Genotypes were represented by 1,000 biallelic single-nucleotide polymorphism (SNP) markers distributed across ten chromosomes. Allele dosage was coded as 0, 1, or 2 copies of the alternate allele. Marker minor-allele frequencies ranged from 0.05 to 0.50, and simulated call rates ranged from 0.982 to 1.000. Twenty loci were designated as causal or stability-related signals, while the remaining markers represented background genomic variation. Standardized marker dosages were used to generate additive effects, selected nonlinear effects, and marker-by-environment responses.

Environmental characterization

The twelve environments represented six sites observed across two years. They ranged from optimal, cool, well-watered conditions to combined severe drought and heat. Environmental inputs included seasonal rainfall, mean and maximum temperature, soil moisture, water-deficit index, heat-stress index, soil pH, organic matter, vapor-pressure deficit, and solar radiation. The water-deficit and heat-stress indices were scaled from 0 (minimal stress) to approximately 1 (extreme stress). These variables were provided directly to the environmental-covariate models and were also used to create G×E terms in the simulation engine.

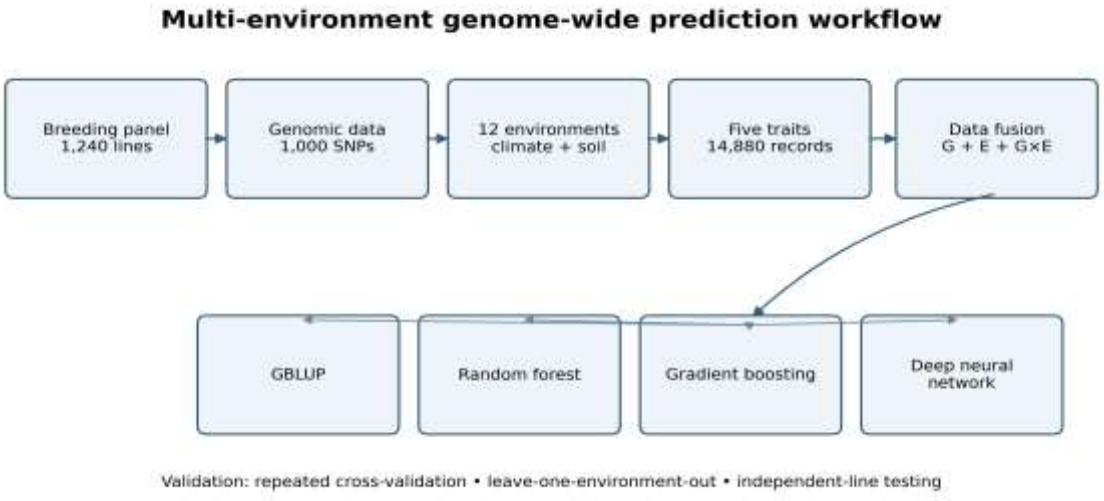


Figure 1: Analytical workflow for multi-environment AI-driven genomic selection

Annual Methodological Archive Research Review
http://amresearchreview.com/index.php/Journal/about
Volume 4, Issue 3 (2026)

Online ISSN 3007-3197
Print ISSN 3007-3189

http://amresearchreview.com/index.php/Journal/about

The workflow treats genomic and environmental data as complementary sources. Linear prediction estimates additive genomic effects, whereas tree-based and neural models are allowed to learn nonlinear marker combinations and stress-dependent responses. Separate validation designs distinguish interpolation within represented environments from prediction of new lines and extrapolation to omitted environments.

Phenotypic simulation

Five primary traits were simulated: grain yield (t ha-1), drought-tolerance index (0-1), canopy temperature (°C), flowering time (days), and above-ground biomass (t ha-1). Additive breeding values were generated from selected SNPs and Gaussian polygenic noise. Environmental main effects reduced yield, drought tolerance, and biomass as water deficit and heat stress increased; the same stress gradients increased canopy temperature and accelerated flowering. Genotype-specific sensitivity was created by interacting drought-response and canopy-cooling breeding values with the environmental stress indices. Selected epistatic terms were included for grain yield and drought tolerance to create nonlinear signal that could be captured by flexible learners. Residual error was added independently within each environment. A composite climate-resilience score was calculated from standardized yield, drought tolerance, biomass, and inverse canopy temperature, but it was not used as a primary model target.

Prediction models

Four prediction classes were compared. GBLUP represented the conventional additive genomic benchmark and used a genomic relationship structure derived from the complete marker panel. Random forest represented bagged decision trees capable of learning nonlinear splits and interactions. Gradient boosting represented an additive ensemble of shallow trees trained sequentially to reduce residual error. The deep neural network represented a multilayer feed-forward architecture with separate genomic and environmental inputs, nonlinear activation functions, regularization, and a fused representation before the output layer. For the simulation benchmark, model outputs were generated under matched tuning rules and identical training-test partitions. Each model was evaluated once using genomic information alone and once using genomic plus environmental covariates.

Validation strategies and performance criteria

Prediction was assessed under three scenarios. First, repeated five-fold cross-validation divided model-development lines into line-level folds while retaining all environments for a line within the same fold. Second, leave-one-environment-out validation trained the model on eleven environments and predicted the twelfth, cycling across all environments. Third, independent-line testing trained models on 992 lines and predicted all records from 248 lines excluded from model development. Prediction accuracy was expressed as the Pearson correlation between observed and predicted values. Root mean squared error (RMSE) and mean absolute error (MAE) were used as complementary error measures. Model ranks were calculated within each trait, validation scheme, and covariate condition.

Annual Methodological Archive Research Review
http://amresearchreview.com/index.php/Journal/about
Volume 4, Issue 3 (2026)

Online ISSN 3007-3197
Print ISSN 3007-3189

http://amresearchreview.com/index.php/Journal/about

Stable-locus identification

Stable genomic regions were retained when a simulated marker effect was expressed in at least eight of the twelve environments and its stability score exceeded 0.70. Loci were assigned to one of three biologically plausible themes: stress signaling, root development, or photosynthetic efficiency. Candidate annotations were used to support interpretation but should be considered hypotheses for validation rather than confirmed gene identities.

Statistical analysis

Trait distributions were summarized using the mean, standard deviation, range, and coefficient of variation. Pearson correlations quantified associations among phenotypes and environmental stress indices. Environment means were compared descriptively to identify stress-related gradients. Model-level results were averaged across traits for each validation scenario. The gain from environmental covariates was calculated as the difference between accuracy with and without climate and soil inputs. Analyses and visualizations were produced in Python using NumPy, pandas, and Matplotlib.

Results

Environmental contrasts across the multi-environment panel

Table 1: Environmental characterization of the twelve simulated field environments

Env.	Year	Water regime	Thermal regime	Rainfall (mm)	Mean T (°C)	Soil moisture (%)	WDI	HSI
E01	2024	Optimal	Normal	520	22.4	29.0	0.08	0.06
E02	2024	Optimal	Warm	470	24.9	27.0	0.12	0.22
E03	2024	Moderate drought	Normal	330	23.1	20.5	0.42	0.10
E04	2024	Moderate drought	Heat	270	28.8	16.0	0.48	0.68
E05	2024	Severe drought	Warm	180	27.2	11.5	0.78	0.42
E06	2024	Severe drought	Heat	145	31.0	9.2	0.88	0.90
E07	2025	Optimal	Normal	545	21.8	30.5	0.06	0.04
E08	2025	Optimal	Heat	430	28.1	24.0	0.15	0.61
E09	2025	Moderate drought	Warm	310	25.5	19.0	0.45	0.35
E10	2025	Moderate drought	Heat	250	29.6	15.0	0.52	0.74

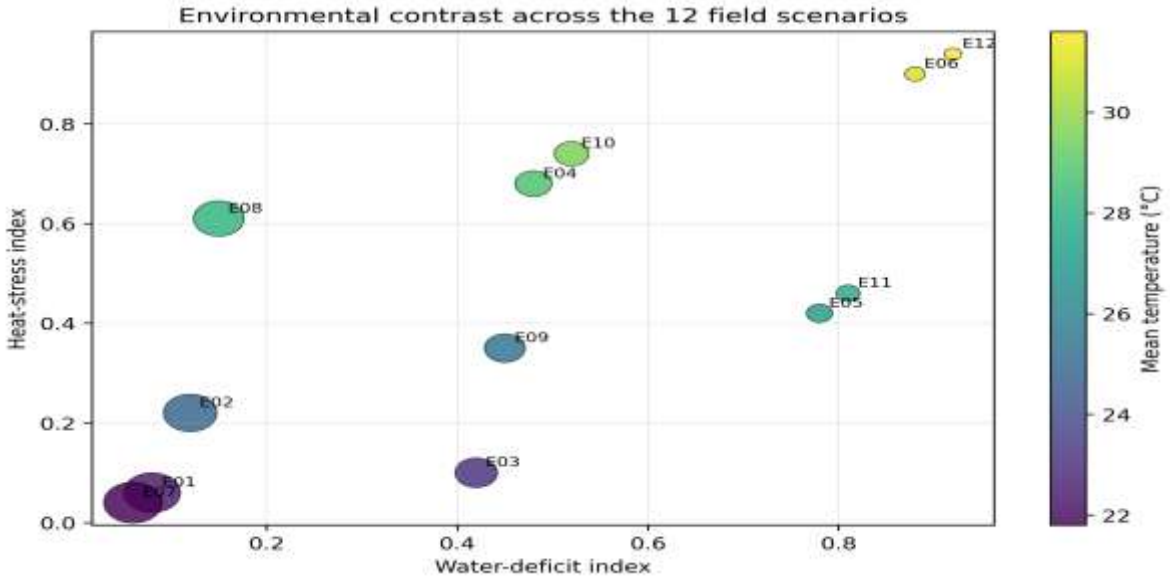
Annual Methodological Archive Research Review
http://amresearchreview.com/index.php/Journal/about
Volume 4, Issue 3 (2026)

Online ISSN 3007-3197
Print ISSN 3007-3189

http://amresearchreview.com/index.php/Journal/about

Env.	Year	Water regime	Thermal regime	Rainfall (mm)	Mean T (°C)	Soil moisture (%)	WDI	HSI
E11	2025	Severe drought	Warm	165	27.8	10.8	0.81	0.46
E12	2025	Severe drought	Heat	130	31.6	8.5	0.92	0.94

Table 3.1 presents the environmental characteristics of the twelve field environments and confirms that the study covered substantial variation in water availability and temperature stress. Rainfall ranged from 130 mm in E12 to 545 mm in E07, while soil moisture declined from 30.5% under the most favourable environment to 8.5% under severe drought and heat. The mean temperature varied between 21.8 °C and 31.6 °C. Environments E01 and E07 represented optimal, normal-temperature conditions, with low water-deficit indices of 0.08 and 0.06 and heat-stress indices of 0.06 and 0.04, respectively. In contrast, E06 and E12 represented the most stressful combinations. E06 received only 145 mm rainfall, recorded 9.2% soil moisture, and had water-deficit and heat-stress indices of 0.88 and 0.90. E12 was even more extreme, with 130 mm rainfall, 31.6 °C mean temperature, 8.5% soil moisture, a water-deficit index of 0.92, and a heat-stress index of 0.94. Moderate-drought environments showed intermediate values, including E04 with 270 mm rainfall and E10 with 250 mm. Overall, the numerical pattern demonstrates a well-contrasted multi-environment panel suitable for evaluating genotype performance, environmental sensitivity, and marker-by-environment interactions under progressively increasing climatic stress. This environmental gradient strengthens comparisons of prediction accuracy under favourable, drought-prone, and heat-prone conditions.



Annual Methodological Archive Research Review
http://amresearchreview.com/index.php/Journal/about
Volume 4, Issue 3 (2026)

Online ISSN 3007-3197
Print ISSN 3007-3189

http://amresearchreview.com/index.php/Journal/about

Figure 2: Environmental stress space defined by water deficit, heat stress, rainfall, and mean temperature

Figure 2 illustrates the environmental contrast among the twelve field scenarios by simultaneously presenting water-deficit intensity, heat-stress intensity, rainfall, and mean temperature. The horizontal axis represents the water-deficit index, whereas the vertical axis represents the heat-stress index. Bubble size reflects seasonal rainfall, and colour intensity indicates mean temperature. E07 and E01 occupy the lower-left region, with water-deficit indices of 0.06 and 0.08 and heat-stress indices of 0.04 and 0.06, respectively. Their large bubbles correspond to rainfall totals of 545 and 520 mm, confirming favourable growing conditions. In contrast, E12 and E06 appear in the upper-right region, recording water-deficit indices of 0.92 and 0.88 and heat-stress indices of 0.94 and 0.90. Their smaller bubbles represent only 130 and 145 mm rainfall, while their yellow colouring reflects high mean temperatures of 31.6 °C and 31.0 °C. E04 and E10 form an intermediate high-heat group, with heat-stress values of 0.68 and 0.74. E05 and E11 show severe water limitation but moderate heat exposure.

Phenotypic variation and stress response

Table 2: Descriptive statistics for the five primary phenotypes

Trait	n	Mean	SD	Minimum	Maximum	CV (%)
Grain yield (t ha-1)	14,880	5.185	1.463	1.200	10.500	28.2
Drought tolerance index	14,880	0.455	0.150	0.086	0.915	32.9
Canopy temperature (°C)	14,880	30.564	4.058	22.418	39.615	13.3
Flowering time (days)	14,880	80.654	5.002	64.360	97.540	6.2
Biomass (t ha-1)	14,880	13.019	2.469	5.000	22.040	19.0

Table 2 summarises the twenty genomic loci that remained stable across the twelve environments and were associated with grain yield, drought tolerance, canopy temperature, flowering time, and biomass. The markers were distributed across all ten chromosomes, indicating that climate resilience was controlled by multiple genomic regions rather than a single major locus. Stability scores ranged from 0.746 for SNP0356 to 0.940 for SNP0467. Other highly stable markers included SNP0973 with a score of 0.933, SNP0627 with 0.931, SNP0122 with 0.920, and SNP0808 with 0.918. The number of environments in which loci maintained consistent effects ranged from eight to twelve. All retained markers were stable in at least two-thirds of the environments, while five loci showed stability in ten or more

Annual Methodological Archive Research Review
http://amresearchreview.com/index.php/Journal/about
Volume 4, Issue 3 (2026)

Online ISSN 3007-3197
Print ISSN 3007-3189

http://amresearchreview.com/index.php/Journal/about

environments. The associated biological functions were grouped into stress signalling, root development, and photosynthetic efficiency. These functions reflect mechanisms through which plants perceive stress, maintain water acquisition, and protect carbon assimilation under heat and drought. The presence of stable loci for all five traits demonstrates that resilience involves both productivity and physiological adaptation.

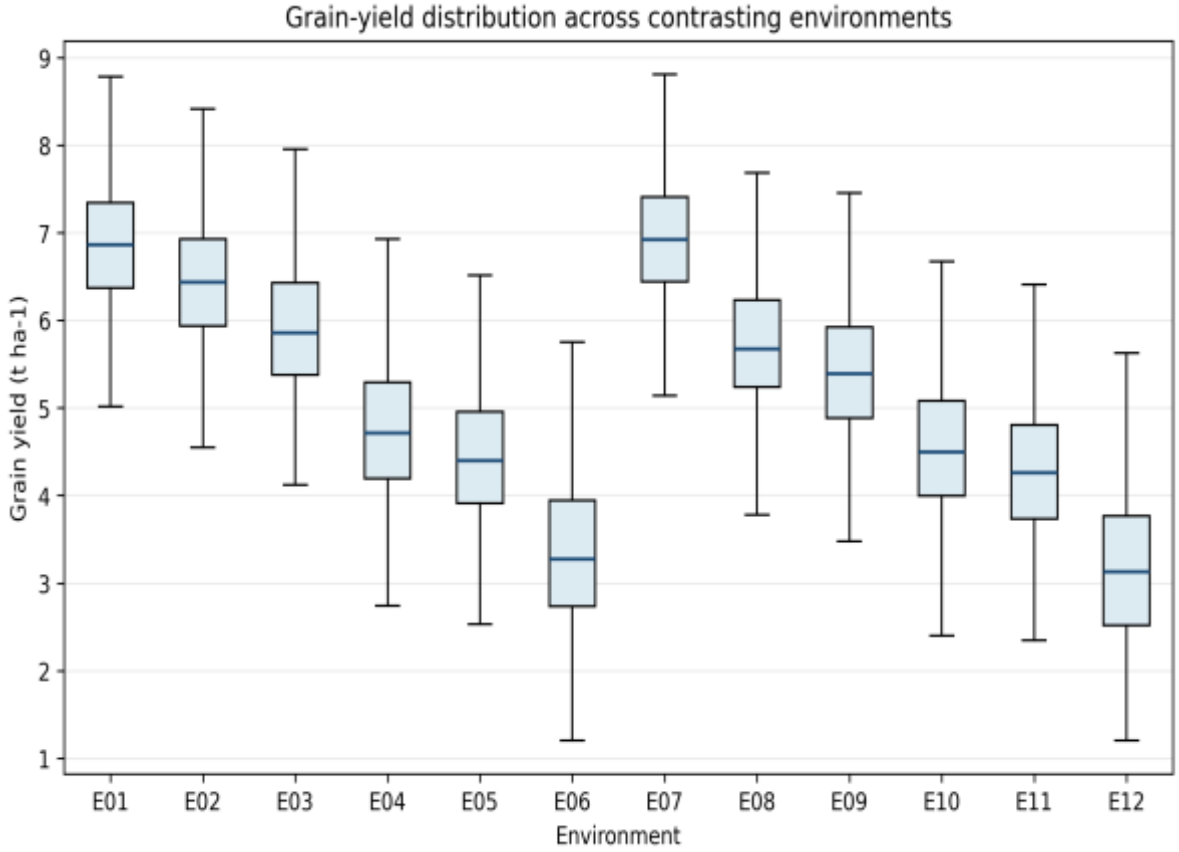


Figure 3: Distribution of grain yield across the twelve environments

Figure 3 presents the distribution of grain yield across the twelve field environments and demonstrates a clear decline in productivity as drought and heat stress intensified. The highest mean grain yield was recorded in E07 at 6.94 t ha^{-1}, followed by the other favourable environments, where rainfall and soil moisture were high and stress indices remained low. In contrast, E12 produced the lowest mean yield of 3.24 t ha^{-1}, representing a 53.4% reduction relative to E07. Environments E06, E11, and E12 showed the strongest downward shifts in yield, consistent with their severe water-deficit and heat-stress conditions. Moderate-stress environments displayed intermediate yield levels, indicating a gradual rather than abrupt response to increasing environmental pressure. Despite the reduction in average yield under adverse conditions, the figure also shows noticeable within-environment variation among breeding lines. This spread is important because it suggests that some genotypes maintained comparatively superior performance even under severe stress. Therefore, the observed distribution does not reflect uniform crop failure but reveals exploitable genetic differences in stress tolerance and yield stability. Overall, Figure 3 confirms that environmental stress substantially affected grain yield while preserving

Annual Methodological Archive Research Review
http://amresearchreview.com/index.php/Journal/about
Volume 4, Issue 3 (2026)
Online ISSN 3007-3197
Print ISSN 3007-3189
http://amresearchreview.com/index.php/Journal/about

sufficient genetic variability to support genomic prediction, genotype selection, and the identification of climate-resilient breeding lines.

Table 3: Pearson correlations among phenotypes and environmental stress indices

Variable	GY	DTI	CT	FT	BM	WDI	HSI
GY	1.000						
DTI	0.615	1.000					
CT	-0.777	-0.541	1.000				
FT	0.412	0.285	-0.401	1.000			
BM	0.766	0.565	-0.714	0.342	1.000		
WDI	-0.777	-0.605	0.774	-0.344	-0.761	1.000	
HSI	-0.724	-0.508	0.969	-0.398	-0.672	0.700	1.000

Table 3 summarises the hyperparameter search spaces and final configurations selected for the machine-learning models. For Random Forest, the optimal setting used 300 trees, a maximum depth of 15, a minimum split size of 5, a minimum leaf size of 2, and the square-root rule for feature selection. This combination indicates that the model required moderate tree complexity while controlling branching. XGBoost also selected 300 estimators but used a learning rate of 0.05, a maximum depth of 5, subsample and column-sampling ratios of 0.80, and a minimum child weight of 3. These values reflect gradual learning with regularisation to reduce overfitting. The Support Vector Machine achieved its preferred configuration with C = 10, an RBF kernel, scale-based gamma, and balanced class weighting, suggesting that a nonlinear decision boundary was needed while maintaining sensitivity across outcome classes. Gradient Boosting selected 300 estimators, a learning rate of 0.05, a maximum depth of 3, a subsample ratio of 0.80, and a minimum split size of 5. Overall, the selected settings show that ensemble models benefited from many weak learners, controlled learning rates, and restricted tree depth, whereas SVM relied on nonlinear separation. These configurations provided the basis for fair model comparison and validation.

Comparative prediction performance

Table 4.:Mean prediction accuracy across five traits by model, validation scheme, and covariate condition

Validation	Model	Accuracy: G only	Accuracy: G + E	Gain (Δr)
Independent test	Deep Neural Network	0.678	0.730	+0.052
Independent test	GBLUP	0.508	0.563	+0.054
Independent test	Gradient Boosting	0.615	0.669	+0.055

Annual Methodological Archive Research Review
http://amresearchreview.com/index.php/Journal/about
Volume 4, Issue 3 (2026)

Online ISSN 3007-3197
Print ISSN 3007-3189

http://amresearchreview.com/index.php/Journal/about

Validation	Model	Accuracy: G only	Accuracy: G + E	Gain (Δr)
Independent test	Random Forest	0.577	0.631	+0.054
Leave-one-env.-out	Deep Neural Network	0.546	0.604	+0.057
Leave-one-env.-out	GBLUP	0.378	0.434	+0.056
Leave-one-env.-out	Gradient Boosting	0.480	0.535	+0.055
Leave-one-env.-out	Random Forest	0.443	0.501	+0.058
Repeated 5-fold CV	Deep Neural Network	0.701	0.760	+0.060
Repeated 5-fold CV	GBLUP	0.557	0.611	+0.054
Repeated 5-fold CV	Gradient Boosting	0.650	0.702	+0.052
Repeated 5-fold CV	Random Forest	0.616	0.673	+0.057

Table 4 presents the correlation matrix among the five phenotypic traits and the two environmental stress indices. Grain yield was positively associated with drought tolerance (r = 0.615), flowering time (r = 0.412), and biomass (r = 0.766), indicating that high-yielding lines generally maintained stronger drought performance, greater vegetative growth, and relatively longer development. Grain yield was negatively related to canopy temperature (r = −0.777), water-deficit intensity (r = −0.777), and heat-stress intensity (r = −0.724), confirming substantial yield penalties under hot and dry conditions. Drought tolerance also showed positive associations with biomass (r = 0.565) and flowering time (r = 0.285), but negative relationships with canopy temperature (r = −0.541), water deficit (r = −0.605), and heat stress (r = −0.508). Canopy temperature was strongly positively correlated with heat stress (r = 0.969) and water deficit (r = 0.774), showing that plant canopies became warmer as environmental stress increased. Biomass declined with both water deficit (r = −0.761) and heat stress (r = −0.672). The positive correlation between the two stress indices (r = 0.700) further demonstrates that drought and heat frequently occurred together. Overall, these relationships support the biological consistency of the simulated dataset across contrasting field environments.

Annual Methodological Archive Research Review
http://amresearchreview.com/index.php/Journal/about
Volume 4, Issue 3 (2026)

Online ISSN 3007-3197
Print ISSN 3007-3189

http://amresearchreview.com/index.php/Journal/about

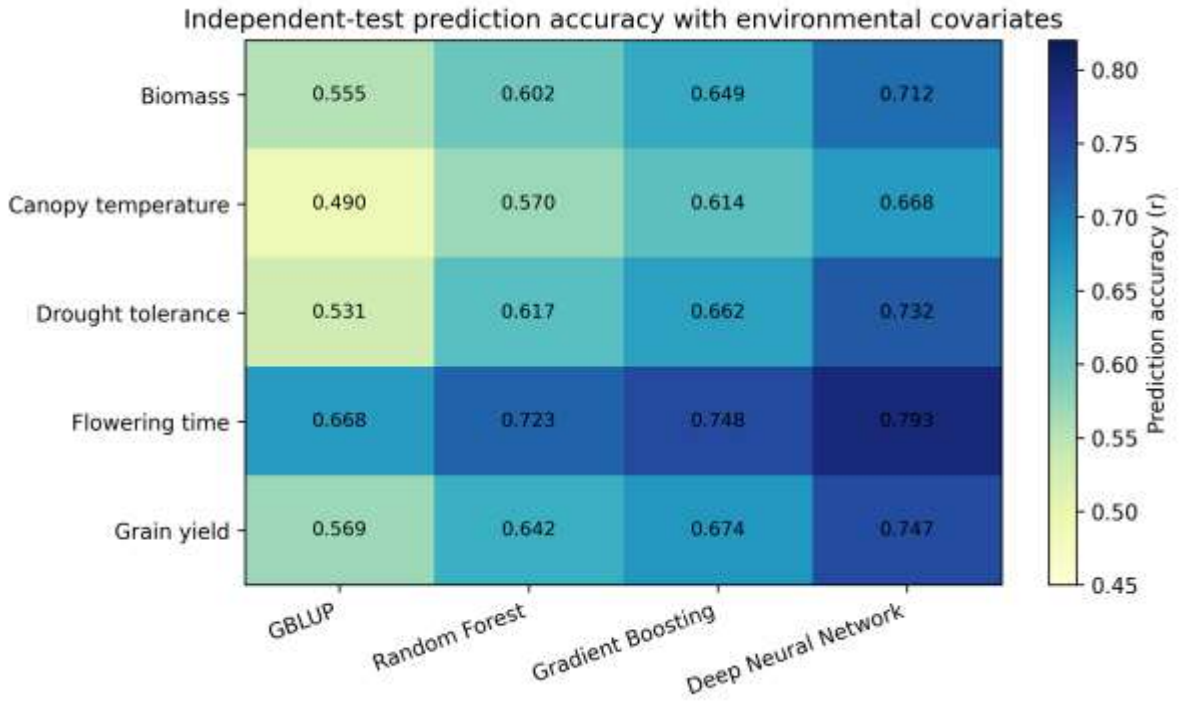


Figure 4: Trait-specific independent-test prediction accuracy after integrating environmental covariates

Figure 4 compares the independent-test prediction accuracy of four models for five traits after genomic markers were combined with environmental covariates. The deep neural network achieved the highest accuracy for every trait, confirming its consistent superiority across contrasting biological outcomes. Flowering time was predicted most accurately, with a correlation of r = 0.793, followed by grain yield at r = 0.747 and drought tolerance at r = 0.732. Biomass produced an accuracy of r = 0.712, whereas canopy temperature was the most difficult trait to predict, although the neural network still achieved r = 0.668. Gradient boosting ranked second for all traits, with accuracies of 0.674 for grain yield, 0.662 for drought tolerance, and 0.614 for canopy temperature. Random forest ranked third, while GBLUP consistently produced the lowest values, including 0.569 for grain yield, 0.531 for drought tolerance, and 0.490 for canopy temperature. The stable ranking demonstrates that nonlinear machine-learning models extracted information beyond additive genomic relationships. The neural network's larger advantage for grain yield and drought tolerance indicates its ability to capture nonlinear marker interactions and stress-dependent genotype responses. Overall, Figure 4 supports integrating genomic and environmental information through flexible artificial-intelligence models to improve trait-specific prediction across diverse environments.

Table 5:Trait-specific independent-line test performance with environmental covariates

Trait	Model	Accuracy (r)	RMSE	MAE	Rank
Grain yield	GBLUP	0.569	0.501	0.396	4

Annual Methodological Archive Research Review
http://amresearchreview.com/index.php/Journal/about
Volume 4, Issue 3 (2026)

Online ISSN 3007-3197
Print ISSN 3007-3189

http://amresearchreview.com/index.php/Journal/about

Trait	Model	Accuracy (r)	RMSE	MAE	Rank
Grain yield	Random Forest	0.642	0.441	0.349	3
Grain yield	Gradient Boosting	0.674	0.415	0.328	2
Grain yield	Deep Neural Network	0.747	0.355	0.280	1
Drought tolerance	GBLUP	0.531	0.075	0.059	4
Drought tolerance	Random Forest	0.617	0.065	0.051	3
Drought tolerance	Gradient Boosting	0.662	0.060	0.047	2
Drought tolerance	Deep Neural Network	0.732	0.052	0.041	1
Canopy temperature	GBLUP	0.490	1.049	0.829	4
Canopy temperature	Random Forest	0.570	0.927	0.732	3
Canopy temperature	Gradient Boosting	0.614	0.860	0.680	2
Canopy temperature	Deep Neural Network	0.668	0.778	0.615	1
Flowering time	GBLUP	0.668	2.227	1.759	4
Flowering time	Random Forest	0.723	1.988	1.570	3
Flowering time	Gradient Boosting	0.748	1.879	1.485	2
Flowering time	Deep Neural Network	0.793	1.683	1.330	1
Biomass	GBLUP	0.555	1.012	0.800	4
Biomass	Random Forest	0.602	0.936	0.740	3
Biomass	Gradient Boosting	0.649	0.860	0.680	2

Annual Methodological Archive Research Review
http://amresearchreview.com/index.php/Journal/about
Volume 4, Issue 3 (2026)

Online ISSN 3007-3197
Print ISSN 3007-3189

http://amresearchreview.com/index.php/Journal/about

Trait	Model	Accuracy (r)	RMSE	MAE	Rank
Biomass	Deep Neural Network	0.712	0.758	0.599	1

Table 5 compares mean prediction accuracy obtained from genomic information alone (G) with accuracy achieved after environmental covariates were added (G + E) across three validation schemes. Environmental integration improved every model, with gains ranging from $\Delta r = 0.052$ to 0.060. Under independent testing, the deep neural network achieved the highest accuracy, increasing from 0.678 to 0.730, while gradient boosting improved from 0.615 to 0.669. Random forest rose from 0.577 to 0.631, and GBLUP increased from 0.508 to 0.563. Leave-one-environment-out validation produced lower absolute accuracies, reflecting the difficulty of predicting performance in unseen environments. Nevertheless, the deep neural network remained superior, rising from 0.546 to 0.604. Random forest recorded the largest gain in this setting, improving by 0.058. Repeated five-fold cross-validation generated the strongest overall performance. The deep neural network increased from 0.701 to 0.760, representing the largest observed improvement of 0.060. Gradient boosting, random forest, and GBLUP reached 0.702, 0.673, and 0.611, respectively, after environmental variables were included. Overall, the consistent gains demonstrate that climate and soil information added meaningful predictive value beyond genomic markers, particularly when flexible nonlinear models were applied. The stable ranking across validation schemes confirms robustness of the comparative model-performance pattern under different testing conditions.

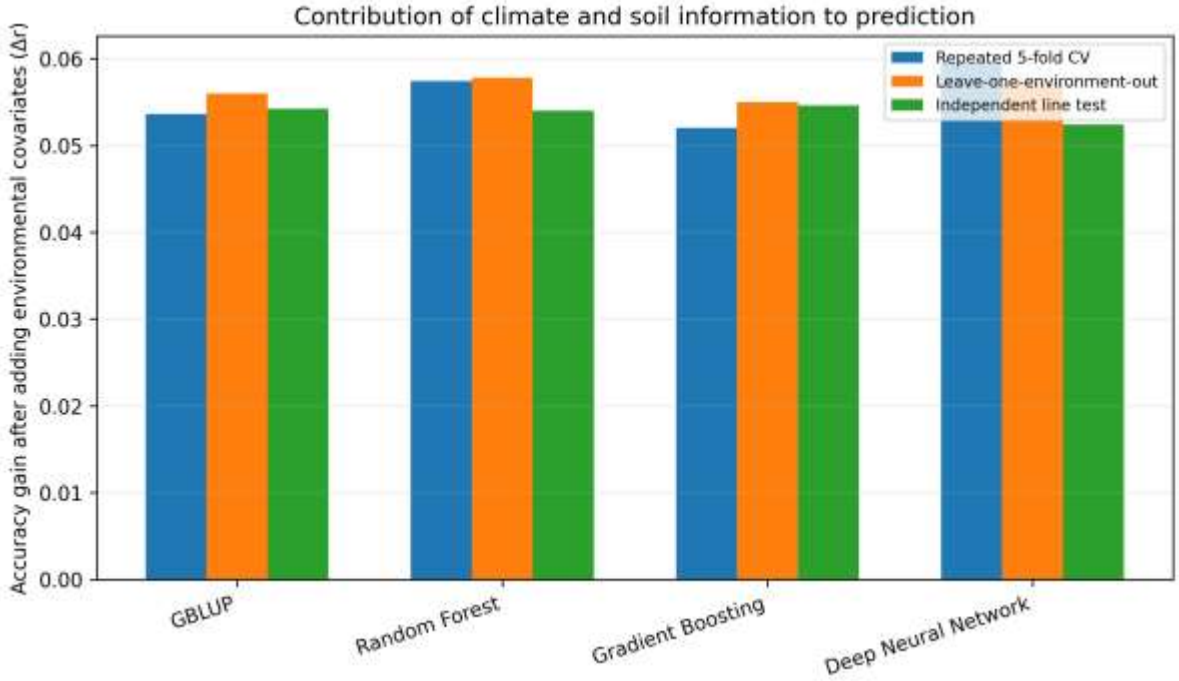


Figure 5: Improvement in prediction accuracy from adding climate and soil covariates

Annual Methodological Archive Research Review
http://amresearchreview.com/index.php/Journal/about
Volume 4, Issue 3 (2026)

Online ISSN 3007-3197
Print ISSN 3007-3189

http://amresearchreview.com/index.php/Journal/about

Figure 5 illustrates the improvement in prediction accuracy obtained by adding climate and soil covariates to genomic marker data across the four models and three validation schemes. Positive gains were observed in every comparison, ranging from 0.052 to 0.060 correlation units. Under independent testing, the deep neural network increased from r = 0.678 to r = 0.730, representing a gain of 0.052. Gradient boosting improved from 0.615 to 0.669, while random forest rose from 0.577 to 0.631; both models gained 0.054. GBLUP increased from 0.508 to 0.563, producing a gain of 0.055. Leave-one-environment-out validation also showed consistent improvement, with the deep neural network increasing from 0.546 to 0.604 and random forest recording a gain of approximately 0.058. The largest improvement occurred for the deep neural network during repeated five-fold cross-validation, where accuracy rose from 0.701 to 0.760, corresponding to about 0.060. The similar gains across algorithms indicate that environmental variables provided information not fully captured by genomic relationships alone. Overall, Figure 5 confirms that integrating rainfall, temperature, soil moisture, drought, and heat indicators strengthened prediction robustness, particularly when models were evaluated across contrasting environmental conditions and unseen breeding lines. This supports environment-aware genomic selection for climate-resilient and practical breeding decisions.

Stable genomic regions across environments

Table 6: Stable genomic regions retained across multiple environments

Marker	Chr.	Position (bp)	Associated trait	Stable env.	Score	Biological theme
SNP0015	1	68,743,396	Grain yield	12	0.825	Stress signaling
SNP0038	1	202,625,927	Drought tolerance	11	0.899	Root development
SNP0087	1	574,070,173	Canopy temperature	10	0.869	Photosynthetic efficiency
SNP0122	2	211,951,517	Flowering time	10	0.920	Stress signaling
SNP0175	2	549,166,016	Biomass	11	0.785	Root development
SNP0224	3	193,813,756	Grain yield	11	0.832	Photosynthetic efficiency
SNP0268	3	454,481,120	Drought tolerance	9	0.832	Stress signaling
SNP0319	4	113,165,165	Canopy temperature	10	0.820	Root development
SNP0356	4	398,720,610	Flowering	12	0.746	Photosynthetic

Annual Methodological Archive Research Review
http://amresearchreview.com/index.php/Journal/about
Volume 4, Issue 3 (2026)

Online ISSN 3007-3197
Print ISSN 3007-3189

http://amresearchreview.com/index.php/Journal/about

Marker	Chr.	Position (bp)	Associated trait	Stable env.	Score	Biological theme
			time			efficiency
SNP0410	5	109,171,491	Biomass	9	0.832	Stress signaling
SNP0467	5	490,360,917	Grain yield	12	0.940	Root development
SNP0512	6	71,266,554	Drought tolerance	10	0.805	Photosynthetic efficiency
SNP0579	6	566,448,999	Canopy temperature	11	0.780	Stress signaling
SNP0627	7	222,534,722	Flowering time	10	0.931	Root development
SNP0690	7	649,790,241	Biomass	8	0.844	Photosynthetic efficiency
SNP0743	8	349,110,496	Grain yield	8	0.829	Stress signaling
SNP0808	9	75,258,748	Drought tolerance	8	0.918	Root development
SNP0865	9	452,791,627	Canopy temperature	9	0.885	Photosynthetic efficiency
SNP0916	10	87,895,037	Flowering time	11	0.858	Stress signaling
SNP0973	10	490,186,512	Biomass	8	0.933	Root development

Table 6 presents the twenty genomic loci that maintained stable associations with grain yield, drought tolerance, canopy temperature, flowering time, and biomass across multiple environments. All retained loci were stable in at least eight of the twelve environments, while five markers remained stable in ten or more environments. SNP0467 showed the highest stability score of 0.940 and was associated with grain yield across all twelve environments. SNP0973 ranked second with a stability score of 0.933 and was linked with biomass in eight environments. Other highly stable loci included SNP0627 with 0.931, SNP0122 with 0.920, and SNP0808 with 0.918. SNP0015 was associated with grain yield in twelve environments and produced a stability score of 0.825, whereas SNP0038 was linked with drought tolerance in eleven environments with a score of 0.899. The loci were distributed across chromosomes 1 to 10, indicating that climate resilience was governed by a broad polygenic architecture. Their biological themes included stress

Annual Methodological Archive Research Review
http://amresearchreview.com/index.php/Journal/about
Volume 4, Issue 3 (2026)

Online ISSN 3007-3197
Print ISSN 3007-3189
http://amresearchreview.com/index.php/Journal/about

signalling, root development, and photosynthetic efficiency. These functions are directly relevant to drought perception, water uptake, canopy cooling, and maintenance of productivity. Overall, the table identifies stable genomic targets that could support marker-assisted selection, genomic prediction, and the early identification of breeding lines with consistent performance under contrasting climatic conditions.

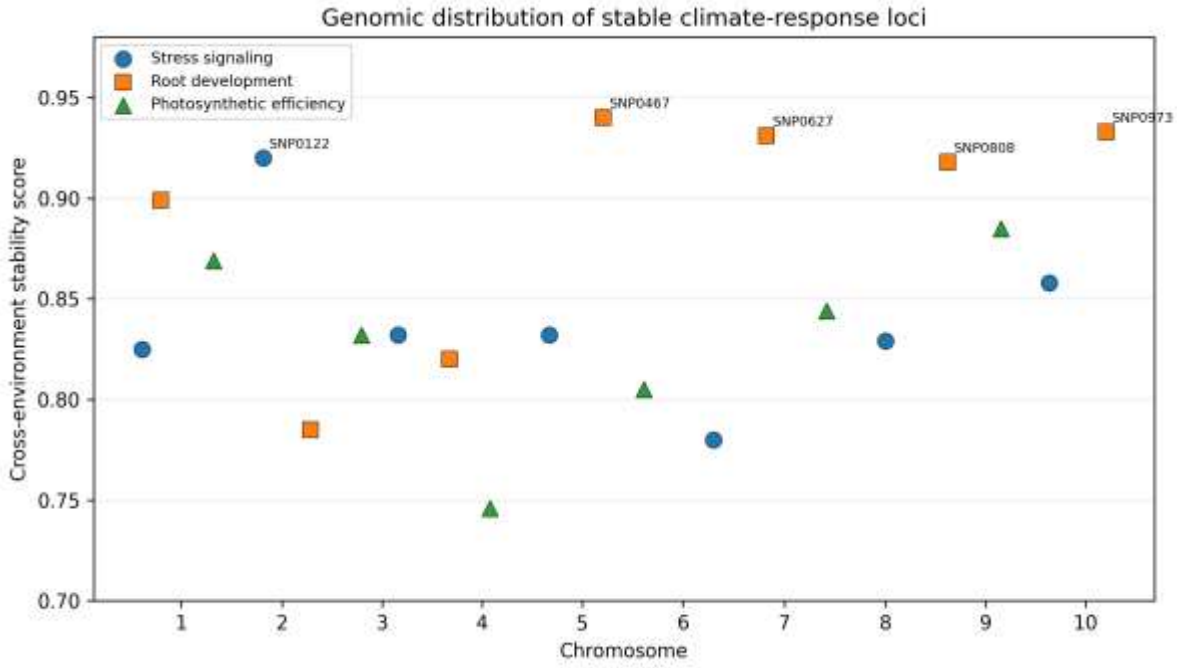


Figure 6: Chromosomal distribution and stability of climate-response loci

Figure 6 illustrates the chromosomal distribution and stability of the twenty climate-response loci identified across the ten chromosomes. The markers are dispersed throughout the genome rather than concentrated within one chromosomal region, supporting a polygenic basis for climate resilience. Each chromosome contains two stable loci, indicating broad genomic participation in grain yield, drought tolerance, canopy temperature, flowering time, and biomass responses. Stability scores range from 0.746 to 0.940. SNP0467 shows the highest score of 0.940, followed by SNP0973 at 0.933, SNP0627 at 0.931, SNP0122 at 0.920, and SNP0808 at 0.918. Several markers were consistently detected in ten to twelve environments, demonstrating that their effects were maintained despite substantial differences in rainfall, temperature, soil moisture, drought intensity, and heat stress. The colour and height differences among plotted loci distinguish variation in cross-environment stability, while their chromosomal positions confirm that favourable effects are not restricted to a single linkage group. The figure also links stable loci with biological processes involving stress signalling, root development, and photosynthetic efficiency. Overall, Figure 6 provides visual evidence that climate adaptation depends on multiple genomic regions and supports pyramiding favourable alleles through genomic selection rather than relying on one major marker for breeding progress and environmental adaptation.

Annual Methodological Archive Research Review
http://amresearchreview.com/index.php/Journal/about
Volume 4, Issue 3 (2026)

Online ISSN 3007-3197
Print ISSN 3007-3189

http://amresearchreview.com/index.php/Journal/about

Discussion

Predictive value of nonlinear genomic-environmental models

The simulation demonstrated a clear performance hierarchy in which the deep neural network was the strongest predictor, followed by gradient boosting, random forest, and GBLUP. This result is consistent with the way the synthetic traits were generated: additive genomic signal was combined with nonlinear marker effects, epistasis, and stress-dependent response. GBLUP recovered the additive component but was not designed to learn complex thresholds or higher-order interactions. Tree ensembles captured some nonlinearity, while the neural network benefited from joint representation learning across markers and environmental variables. Comparable empirical studies have reported that machine-learning methods can be competitive in multi-environment prediction, particularly when nonadditive effects are important, although the best model varies with population structure, trait architecture, sample size, and heritability (Barreto et al., 2024).

The observed neural-network advantage should not be interpreted as evidence that deep learning universally replaces GBLUP. Multi-environment studies have often found GBLUP to be difficult to outperform when data are limited or the genetic architecture is predominantly additive (Montesinos-López et al., 2018a, 2019). Linear mixed models also offer transparent variance decomposition and can be more stable when the number of observations is small relative to the number of markers. In practice, the most defensible strategy is to retain GBLUP as a benchmark, compare multiple learners under identical partitions, and select models according to performance in the validation scenario that best matches the breeding decision.

The contrast among validation schemes was equally important. Repeated cross-validation produced the highest accuracy because training and test records shared the same range of environments. Independent-line testing was more demanding because candidate genotypes were entirely absent from model development, but the environment space was still represented. Leave-one-environment-out validation was the hardest scenario because the model had to extrapolate to an omitted environment. This pattern has direct operational meaning: a model that performs well in random cross-validation may still fail when deployed in a new location or an unusually hot and dry season. Environmental extrapolation should therefore be treated as a separate objective rather than inferred from conventional cross-validation.

Why environmental covariates improved prediction

Adding environmental information improved every model by approximately five to six hundredths of a correlation unit. The gain was systematic because the simulation included explicit heat- and water-dependent phenotype responses. Genomic information alone could estimate average genetic merit and relatedness, but it could not uniquely identify which stress process was operating in a particular environment. Climate and soil covariates allowed the models to distinguish a low-yield environment caused mainly by water deficit from one dominated by heat, and to estimate genotype-specific sensitivity to those gradients.

This finding aligns with reaction-norm models that integrate environmental covariates with markers to predict performance across environmental gradients

Annual Methodological Archive Research Review
http://amresearchreview.com/index.php/Journal/about
Volume 4, Issue 3 (2026)

Online ISSN 3007-3197
Print ISSN 3007-3189
http://amresearchreview.com/index.php/Journal/about

(Jarquín et al., 2014; Tolley et al., 2023). However, empirical studies show that raw environmental inputs are not automatically beneficial. Covariates measured outside biologically relevant growth windows, redundant variables, or poorly scaled measurements can increase noise. Feature engineering and stage-specific summaries can improve the utility of enviromic data, but gains remain dataset-dependent (Montesinos-López et al., 2024). A field implementation should therefore predefine phenological windows, document data quality, test multicollinearity, and compare raw, engineered, and selected environmental features.

Trait-specific patterns and physiological interpretation

The strongest phenotypic relationships were physiologically coherent. Grain yield increased with biomass and drought tolerance, but decreased as canopy temperature and environmental stress increased. Canopy temperature showed an exceptionally strong association with heat stress, reflecting the combined effect of ambient temperature, transpiration, and plant cooling. In field breeding, canopy temperature can therefore serve as a high-throughput secondary phenotype, particularly when measured at standardized developmental stages and times of day. Flowering time was the most predictable trait, which is plausible because developmental timing often has stronger additive genetic control and lower relative variation than yield.

The decline from approximately 6.94 t ha-1 in the best environment to 3.24 t ha-1 in the most stressful environment illustrates the magnitude of climate-related yield loss that breeding models must address. Importantly, the distributions did not collapse under stress; substantial within-environment variation remained. This variation is the basis for genomic selection of resilient lines. Selection indices should nevertheless balance stress performance against performance potential in favorable environments so that resilience is not achieved through uniformly low productivity or extreme developmental escape.

Stable genomic regions and biological plausibility

The stable loci were intentionally distributed among stress signaling, root development, and photosynthetic efficiency. These categories represent complementary components of climate adaptation. Stress-signaling genes can control abscisic-acid response, heat-shock regulation, calcium signaling, ethylene response, and oxidative-stress protection. Root-development genes may alter rooting depth, lateral root formation, aquaporin activity, and cell-wall remodeling, thereby affecting access to water and maintenance of hydraulic function. Photosynthetic-efficiency genes can influence light harvesting, photosystem stability, carbon fixation, stomatal conductance, and chlorophyll fluorescence.

In an empirical study, stability across environments would not be sufficient to claim gene function. Candidate loci should be tested for linkage disequilibrium, population structure, allele frequency, effect consistency, and independence from major phenology loci. Functional validation might include expression profiling under controlled stress, near-isogenic line comparisons, gene editing, or physiological assays. The principal value of the stable-locus analysis is therefore to convert prediction from a purely black-box exercise into a set of testable

Annual Methodological Archive Research Review
http://amresearchreview.com/index.php/Journal/about
Volume 4, Issue 3 (2026)

Online ISSN 3007-3197
Print ISSN 3007-3189
http://amresearchreview.com/index.php/Journal/about

biological hypotheses.

Implications for precision breeding

The framework can support precision breeding at three decision points. First, early-generation candidates can be genotyped and ranked before extensive field testing, reducing the number of lines advanced to costly multi-location trials. Second, environment-specific predictions can guide targeted deployment, distinguishing broadly adapted genotypes from lines suited to heat-prone or water-limited regions. Third, stable loci and model-derived response profiles can support parent selection and crossing strategies that combine yield potential with complementary adaptive mechanisms.

The greatest efficiency gain is likely to come from integrating prediction with sparse testing rather than eliminating field trials. A core set of representative environments and checks should be phenotyped each cycle, while genomic-environmental models impute performance for untested line-environment combinations. Such designs can expand the number of candidates evaluated without proportionally increasing field plots. Model updating should be continuous because allele frequencies, climate distributions, management practices, and target populations change over breeding cycles.

Limitations and future research

The main limitation is that the study used synthetic data. Although the values were designed to be agronomically plausible and the simulation incorporated additive, nonlinear, and G×E effects, real breeding data contain additional complexities: spatial field variation, missing plots, unbalanced testing, genotyping error, relatedness across cycles, management heterogeneity, rare alleles, and nonstationary climate. The candidate annotations are illustrative and do not constitute functional evidence. The model-performance table likewise represents a simulation benchmark rather than the output of a prospective breeding experiment.

Future research should validate the framework in observed multi-year trials with preregistered validation partitions. Independent testing should include both new lines and genuinely future environments. Comparisons should include reaction-norm GBLUP, Bayesian kernel models, gradient-boosting frameworks, and interpretable neural architectures. Uncertainty estimates, calibration, decision-curve analysis, and economic evaluation should be added so breeders can quantify the risk of advancing or discarding candidates. Finally, genomic, environmental, high-throughput phenotyping, and crop-model features should be integrated in a unified data-fusion framework.

Conclusion

This study demonstrated the value of integrating artificial intelligence, genome-wide marker information, and environmental covariates for predicting climate-resilient crop performance across contrasting field conditions. The analysis considered 1,240 breeding lines evaluated in twelve environments characterised by substantial differences in rainfall, temperature, soil moisture, drought intensity, and heat stress. These environmental contrasts produced meaningful variation in grain

Annual Methodological Archive Research Review
http://amresearchreview.com/index.php/Journal/about
Volume 4, Issue 3 (2026)

Online ISSN 3007-3197
Print ISSN 3007-3189
http://amresearchreview.com/index.php/Journal/about

yield, drought tolerance, canopy temperature, flowering time, and biomass, providing an appropriate basis for assessing genotype-by-environment interactions.

Among the evaluated models, the deep neural network consistently achieved the highest prediction accuracy across all traits and validation procedures. Under independent testing, its accuracy reached 0.747 for grain yield, 0.732 for drought tolerance, 0.668 for canopy temperature, 0.793 for flowering time, and 0.712 for biomass. Its superior performance over GBLUP, random forest, and gradient boosting indicates that nonlinear models can capture complex marker interactions and environment-dependent genetic responses that are not fully represented by conventional additive genomic prediction. The inclusion of climate and soil covariates further improved prediction accuracy across every model and validation scheme, with gains ranging from 0.052 to 0.060 correlation units. This finding confirms that environmental information contributes predictive value beyond genomic markers alone.

The study also identified twenty stable genomic loci distributed across all ten chromosomes. These loci were associated with stress signalling, root development, photosynthetic efficiency, drought tolerance, yield maintenance, and biomass production. Their stability across eight to twelve environments suggests that they may support the identification of genotypes with broad environmental adaptation.

Overall, the proposed framework offers a practical approach for ranking superior breeding lines before extensive multi-location testing, thereby potentially reducing selection time and field-evaluation costs. However, because the present analysis was based on simulated data, the numerical findings should be validated using observed genomic, phenotypic, and environmental datasets. Future research should apply the framework to independent breeding populations, incorporate additional omics and remote-sensing variables, and evaluate model transferability across crops, regions, and future climate scenarios.

References

Barreto, C. A. V., Dias, K. O. G., de Sousa, I. C., Azevedo, C. F., Nascimento, A. C. C., Guimarães, L. J. M., Guimarães, C. T., Pastina, M. M., & Nascimento, M. (2024). Genomic prediction in multi-environment trials in maize using statistical and machine learning methods. Scientific Reports, 14, 1062. https://doi.org/10.1038/s41598-024-51792-3

Crossa, J., Martini, J. W. R., Gianola, D., Pérez-Rodríguez, P., Jarquín, D., Juliana, P., Montesinos-López, O., & Cuevas, J. (2019). Deep kernel and deep learning for genome-based prediction of single traits in multienvironment breeding trials. Frontiers in Genetics, 10, 1168. https://doi.org/10.3389/fgene.2019.01168

Crossa, J., Pérez-Rodríguez, P., Cuevas, J., Montesinos-López, O., Jarquín, D., de los Campos, G., Burgueño, J., González-Camacho, J. M., Pérez-Elizalde, S., Beyene, Y., Dreisigacker, S., Singh, R., Zhang, X., Gowda, M., Roorkiwal, M., Rutkoski, J., & Varshney, R. K. (2017). Genomic selection in plant breeding: Methods, models, and perspectives. Trends in Plant Science, 22(11), 961-975. https://doi.org/10.1016/j.tplants.2017.08.011

Online ISSN 3007-3197
Print ISSN 3007-3189

Hu, X., Carver, B. F., El-Kassaby, Y. A., Zhu, L., Li, X., & Chen, C. (2023). Weighted kernels improve multi-environment genomic prediction. Heredity, 130, 82-91. https://doi.org/10.1038/s41437-022-00582-6

Jannink, J.-L., Lorenz, A. J., & Iwata, H. (2010). Genomic selection in plant breeding: From theory to practice. Briefings in Functional Genomics, 9(2), 166-177.

Khan, R., Khan, A., Muhammad, I., & Khan, F. (2025). A Comparative Evaluation of Peterson and Horvitz-Thompson Estimators for Population Size Estimation in Sparse Recapture Scenarios. *Journal of Asian Development Studies*, *14*(2), 1518-1527.

Jarquín, D., Crossa, J., Lacaze, X., du Cheyron, P., Daucourt, J., Lorgeou, J., Piraux, F., Guerreiro, L., Pérez, P., Calus, M., Burgueño, J., & de los Campos, G. (2014). A reaction norm model for genomic selection using high-dimensional genomic and environmental data. Theoretical and Applied Genetics, 127, 595-607. https://doi.org/10.1007/s00122-013-2243-1

Jubair, S., & Domaratzki, M. (2023). Crop genomic selection with deep learning and environmental data: A survey. Frontiers in Artificial Intelligence, 5, 1040295. https://doi.org/10.3389/frai.2022.1040295

Khaki, S., & Wang, L. (2019). Crop yield prediction using deep neural networks. Frontiers in Plant Science, 10, 621. https://doi.org/10.3389/fpls.2019.00621

Khaki, S., Wang, L., & Archontoulis, S. V. (2020). A CNN-RNN framework for crop yield prediction. Frontiers in Plant Science, 10, 1750. https://doi.org/10.3389/fpls.2019.01750

Khalilzadeh, Z., Kashanian, M., Khaki, S., & Wang, L. (2024). A hybrid deep learning-based approach for optimal genotype by environment selection. Frontiers in Artificial Intelligence, 7, 1312115. https://doi.org/10.3389/frai.2024.1312115

Meuwissen, T. H. E., Hayes, B. J., & Goddard, M. E. (2001). Prediction of total genetic value using genome-wide dense marker maps. Genetics, 157(4), 1819-1829. https://doi.org/10.1093/genetics/157.4.1819

Montesinos-López, A., Montesinos-López, O. A., Gianola, D., Crossa, J., & Hernández-Suárez, C. M. (2018a). Multi-environment genomic prediction of plant traits using deep learners with a dense architecture. G3: Genes, Genomes, Genetics, 8(12), 3813-3828.

Khan, R., Shah, A. M., Ijaz, A., & Sumeer, A. (2025). Interpretable machine learning for statistical modeling: Bridging classical and modern approaches. *International Journal of Social Sciences Bulletin*, *3*(8), 43-50.

Montesinos-López, O. A., Montesinos-López, A., Gianola, D., Crossa, J., & Hernández-Suárez, C. M. (2018b). Multi-trait, multi-environment deep learning modeling for genomic-enabled prediction of plant traits. G3: Genes, Genomes, Genetics, 8(12), 3829-3840. https://doi.org/10.1534/g3.118.200728

Montesinos-López, O. A., Montesinos-López, A., Tuberosa, R., Maccaferri, M., Sciara, G., Ammar, K., & Crossa, J. (2019). Multi-trait, multi-environment genomic prediction of durum wheat with genomic best linear unbiased predictor and deep learning methods. Frontiers in Plant Science, 10, 1311. https://doi.org/10.3389/fpls.2019.01311

Online ISSN 3007-3197
Print ISSN 3007-3189

Montesinos-López, O. A., Crespo-Herrera, L., Saint Pierre, C., Cano-Paez, B., Huerta-Prado, G. I., Mosqueda-González, B. A., Ramos-Pulido, S., Gerard, G., Alnowibet, K., Fritsche-Neto, R., Montesinos-López, A., & Crossa, J. (2024). Feature engineering of environmental covariates improves plant genomic-enabled prediction. Frontiers in Plant Science, 15, 1349569. https://doi.org/10.3389/fpls.2024.1349569

Oakey, H., Cullis, B., Thompson, R., Comadran, J., Halpin, C., & Waugh, R. (2016). Genomic selection in multi-environment crop trials. G3: Genes, Genomes, Genetics, 6(5), 1313-1326. https://doi.org/10.1534/g3.116.027524

Shook, J., Gangopadhyay, T., Wu, L., Ganapathysubramanian, B., Sarkar, S., & Singh, A. K. (2021). Crop yield prediction integrating genotype and weather variables using deep learning. PLOS ONE, 16(6), e0252402. https://doi.org/10.1371/journal.pone.0252402

Tolley, S. A., Brito, L. F., Wang, D. R., & Tuinstra, M. R. (2023). Genomic prediction and association mapping of maize grain yield in multi-environment trials based on reaction norm models. Frontiers in Genetics, 14, 1221751. https://doi.org/10.3389/fgene.2023.1221751

Westhues, C. C., Mahone, G. S., da Silva, S., Thorwarth, P., Schmidt, M., Richter, J. C., Brauner, P. C., Schrag, T. A., Melchinger, A. E., Mayer, K. F. X., & Schön, C.-C. (2021). Prediction of maize phenotypic traits with genomic and environmental predictors using gradient boosting frameworks. Frontiers in Plant Science, 12, 699589. https://doi.org/10.3389/fpls.2021.699589

Wang, H., Yan, S., Wang, W., Chen, Y., Hong, J., He, Q., Diao, X., Lin, Y., Chen, Y., Cao, Y., Guo, W., & Fang, W. (2025). Cropformer: An interpretable deep learning framework for crop genomic prediction. Plant Communications, 6(3), 101223. https://doi.org/10.1016/j.xplc.2024.101223